Impact of Greenland and Antarctic ice sheet interactions on climate sensitivity

H. Goelzer · P. Huybrechts · M. F. Loutre ·
H. Goosse · T. Fichefet · A. Mouchet

Abstract We use the Earth system model of intermediate complexity LOVECLIM to show the effect of coupling interactive ice sheets on the climate sensitivity of the model on a millennial time scale. We compare the response to a $2 \times CO_2$ warming scenario between fully coupled model versions including interactive Greenland and Antarctic ice sheet models and model versions with fixed ice sheets. For this purpose an ensemble of different parameter sets have been defined for LOVECLIM, covering a wide range of the model's sensitivity to greenhouse warming, while still simulating the present-day climate and the climate evolution over the last millennium within observational uncertainties. Additional freshwater fluxes from the melting ice sheets have a mitigating effect on the model's temperature response, leading to generally lower climate sensitivities of the fully coupled model versions. The mitigation is effectuated by changes in heat exchange within the ocean and at the sea–air interface, driven by freshening of the surface ocean and amplified by sea–ice-related feedbacks. The strength of the effect depends on the response of the ice sheets to the warming and on the model's climate sensitivity itself. The effect is relatively strong in model versions with higher climate sensitivity due to the relatively large polar amplification of LOVEC-LIM. With the ensemble approach in this study we cover a wide range of possible model responses.

1 Introduction

Uncertainties on future sea-level rise and the important role of the continental cryosphere have recently drawn a lot of attention to coupled ice sheet-climate modelling. Currently only a few global climate models exist that include dynamically coupled models for the Greenland (e.g. Ridley et al. 2005; Calov et al. 2005) and/or Antarctic ice sheets (e.g. Driesschaert et al. 2007; Mikolajewicz et al. 2007a). It is however likely that the future will see more development work in this direction, as interactions between ice sheets on the one side and atmosphere and ocean on the other side are expected to highlight the important role of feedback mechanisms, making it necessary to examine the fully coupled system.

Some authors have studied future ice sheet-climate interactions with both atmosphere and ocean (Ridley et al. 2005; Driesschaert et al. 2007; Mikolajewicz et al. 2007b; Vizcaíno et al. 2008, 2010; Swingedouw et al. 2008); others have focused especially on feedbacks with the ocean (Huybrechts et al. 2002; Fichefet et al. 2003). Interactions with the atmosphere include changes in precipitation and heat fluxes due to the temporal evolution of surface elevation and albedo. It has been shown that the ice-albedo feedback for Greenland starts to become important for the total mass balance when the ice sheet is considerably reduced in volume (and area), with an estimated threshold of 3/4 (Vizcaíno et al. 2008) of the original volume.

H. Goelzer (✉) · P. Huybrechts
Earth System Sciences and Departement Geografie,
Vrije Universiteit Brussel, Brussels, Belgium
e-mail: heiko.goelzer@vub.ac.be

M. F. Loutre · H. Goosse · T. Fichefet
Georges Lemaître Centre for Earth
and Climate Research (TECLIM), Earth and Life Institute,
Université catholique de Louvain, Louvain-la-Neuve, Belgium

A. Mouchet
Laboratoire de Physique Atmosphérique et Planétaire,
Université de Liège, Liège, Belgium

Modelling studies suggest that freshwater fluxes from the Greenland ice sheet have the potential to weaken the Atlantic meriodional overturning circulation (MOC), with consequences for the heat budget of the northern North Atlantic ocean and consequently also for Greenland surface temperatures (e.g. Huybrechts et al. 2002; Fichefet et al. 2003). The feedback between ice sheet and ocean is in principle effectuated by freshwater fluxes from the melting ice sheet that alter the oceanic density structure, the heat exchange within the water column and with the atmosphere, and ultimately the large scale ocean circulation. As a result, a local relative cooling in the North Atlantic sector occurs, which is further amplified by sea–ice-related feedbacks. The magnitude of the MOC response to freshwater perturbations however varies strongly among existing models (e.g. Stouffer et al. 2006). Additionally, it has been shown that MOC weakening in future greenhouse warming simulations can also be caused by other factors, such as changes in the sea-air temperature difference or enhanced northward atmospheric moisture transport (e.g. Rahmstorf and Ganopolski 1999; Gregory et al. 2005; Winguth et al. 2005; Mikolajewicz et al. 2007b).

For a strong, 3,000 years warming scenario, which causes a considerable amount of melting of the Antarctic ice sheet, Swingedouw et al. (2008) found a melt water induced negative feedback mechanism similar to the one in the Northern Hemisphere described above that led to a relative global cooling. In their experiments, melt water fluxes perturb the Antarctic surface waters, leading to a stronger halocline with reduced vertical heat exchange and local cooling that is further amplified by sea–ice interactions.

We use an Earth system model of intermediate complexity (EMIC) to study the effect of including fully interactive ice sheets under greenhouse warming conditions on the millennial time scale. The use of a computationally efficient EMIC allows us to perform a large number of experiments with different parameter combinations. In this way we are able to cover a wide range of possible model responses to greenhouse warming, which is complementary to the usual approach of forcing one model with different forcing scenarios (e.g. Johns et al. 2003; Nakashiki et al. 2006). Limitations of the EMIC with consequences for the results of this study are mainly related to simplifications in the atmospheric component and its relatively low resolution. This both necessitates a coupling of the ice sheet models in anomaly mode and is the main reason for relatively high polar amplification factors.

A common practice with coupled ocean–atmosphere models of low resolution, like the one used in this study, is to integrate them with constant external forcing in order to reach a steady state, e.g. for the preindustrial climate, as starting point for transient climate simulations. The underlying assumption is that both atmosphere and ocean have a short enough memory, so that the equilibrium state is well suited as a starting point for transient simulations. One new aspect however when using models including interactive ice sheets with a response time scale of thousands of years, is the fact that equilibrium simulations for a given climate cannot be evaluated. Consequently, the IPCC AR4 definition of 'equilibrium climate sensitivity' (Randall et al. 2007) cannot be applied. Since we are interested in the climate sensitivity of our model on a millennial time scale including the dynamic effect of the ice sheets, the alternative definition of 'effective climate sensitivity' (Murphy 1995) is used. It is calculated on the basis of the global mean surface temperature change, oceanic heat storage and radiative forcing (Cubasch et al. 2001; Gregory et al. 2002) for a stabilized $2\times CO_2$ scenario after 1,000 years. We thus focus our analysis on a model state where both major ice sheets are still present and potentially contribute to climate feedbacks.

The manuscript continues as follows: we first describe the model (Sect. 2) and the experimental setup (Sect. 3). We introduce our measure for climate sensitivity (Sect. 4) and describe the parameter selection for the model ensemble (Sect. 5). Results are presented in Sect. 6, followed by a discussion (Sect. 7) and conclusions (Sect. 8).

2 Model description

In this study we use the Earth system model of intermediate complexity LOVECLIM 1.1 (Goosse et al. 2007), a further development of version 1.0 (Driesschaert et al. 2007; Swingedouw et al. 2008) and largely similar to version 1.2 (Goosse et al. 2010). It includes components for the atmosphere (ECBilt), the ocean and sea–ice (CLIO), the terrestrial biosphere (VECODE), the carbon cycle (LOCH) and the ice sheets (AGISM). Figure 1 schematically shows all model components and their mutual interactions. In the following we will refer to the fully coupled model as LOVECLIM, which we compare to a version without interactive ice sheets (ECVL). Extent and surface elevation of the ice sheets in ECVL are prescribed and precipitation over ice sheet area is treated similar to the rest of the continents.

ECBilt (Opsteegh et al. 1998) is a spectral atmospheric model with truncation T21, which corresponds approximately to a horizontal resolution of 5.625° in longitude and latitude, and incorporates three vertical levels. It includes simple parameterizations of the diabatic heating processes and an explicit representation of the hydrological cycle. Cloud cover is prescribed according to present-day climatology, which is a limitation of the present study. Coupled large-scale ice-ocean model (CLIO) is a global free-surface
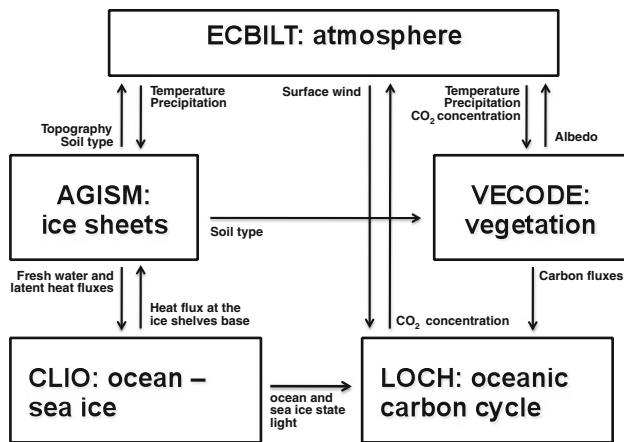
Fig. 1 Scheme of the interactions between the various LOVECLIM components. For clarity, the ocean–atmosphere interactions are omitted. The following quantities are exchanged between ocean and atmosphere: wind stress, sea surface temperature, radiative, turbulent and freshwater fluxes, albedo, thickness and fractions of sea–ice and snow

ocean general circulation model coupled to a thermodynamic sea–ice model (Fichefet and Morales Maqueda 1997; Goosse and Fichefet 1999; Goosse et al. 1999). The horizontal resolution of CLIO is 3° in longitude and latitude, and there are 20 unevenly spaced levels in the vertical. VEgetation COntinuous DEscription model (VECODE) is a reduced-form model of the vegetation dynamics and of the terrestrial carbon cycle (Brovkin et al. 1997). It is based on a continuous bioclimatic classification: every land grid cell is covered by a mixture of grass, forest and desert. Liège Ocean Carbon Heteronomous model (LOCH) (Mouchet and François 1996) is a comprehensive, three-dimensional oceanic carbon cycle model. Since the evolution of CO_2 concentration was prescribed in the present simulations, the carbon cycle component of the model was used in diagnostic mode and its results are not discussed here.

Antarctic and Greenland Ice Sheet Model (AGISM) (Huybrechts 1990, 1996; Huybrechts and de Wolde 1999) consists of two–three-dimensional thermomechanical ice-dynamic models for each of the polar ice sheets [Greenland Ice Sheet (GIS) and Antarctic ice sheet (AIS)]. Both models are based on the same physics and formulations, however, with one major distinction: the AIS model incorporates coupled ice shelf and grounding line dynamics. For the GIS these issues can be omitted, as there is hardly any floating ice at present, let alone in warmer conditions. Having a melt margin on land or a calving margin close to the coastline for most of its glacial history, ice shelves probably played a minor role in Greenland also during colder conditions.

Both polar ice sheet models consist of three main components that represent the ice flow, the mass balance at the ice-atmosphere and ice-ocean interfaces and the solid
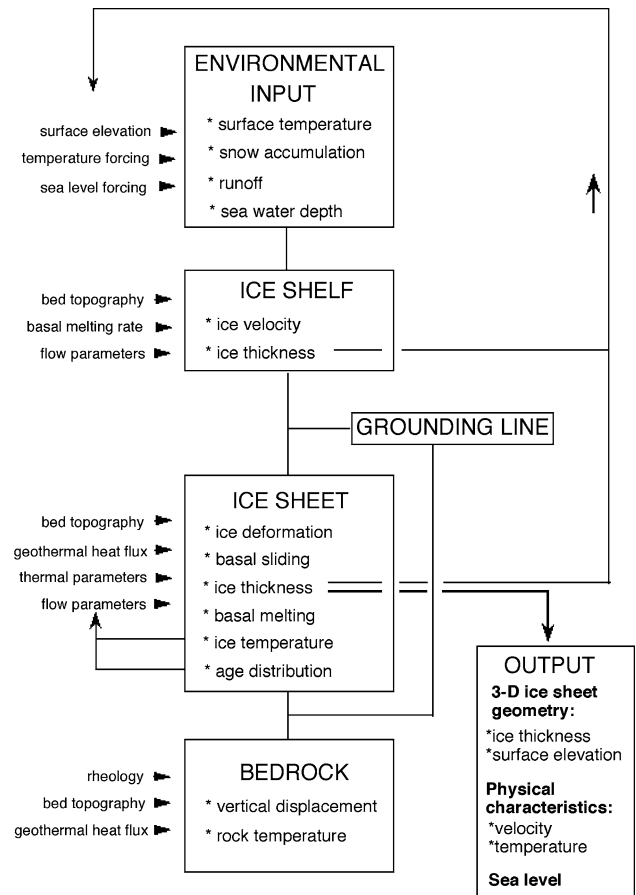

Fig. 2 Structure of the three-dimensional thermodynamic ice sheet model AGISM. The inputs are given at the *left side*. Prescribed environmental variables drive the model, which incorporates ice shelves, grounded ice and bed adjustment as its major components. Regarding the Antarctic component, the position of the grounding line is not prescribed, but internally generated. The model essentially outputs the time-dependent ice sheet geometry and the associated temperature and velocity fields

Earth response (Huybrechts and de Wolde 1999; Huybrechts 2002). Figure 2 displays the general structure of the ice sheet models. At the heart of these models lies the simultaneous integration of evolutionary equations for ice thickness and temperature, together with diagnostic representations for ice velocity. Grounded ice flow is due to internal deformation and, if basal temperatures reach the pressure melting point, to sliding over the bed in the presence of a lubricating water layer. Ice deformation in the ice sheet domain results from vertical shearing, most of which occurs near to the base. Longitudinal deviatoric stresses are disregarded according to the widely used 'Shallow Ice Approximation'. This does not treat the rapid component of the otherwise badly understood physics specific to the acceleration of fast-flowing outlet glaciers or ice streams. A flow law of 'Glen type' is used with exponent $n = 3$. The temperature dependence of the rate factor is represented by an exponential Arrhenius equation:

$$A(T^*) = m \, a \, \exp\left\{\frac{-Q}{RT^*}\right\} \tag{1}$$

where a is specified below, R is the gas constant (8.314 J/mol/K), Q the activation energy for creep, T^* the absolute temperature corrected for the dependence of the melting point on pressure and m an enhancement factor used as tuning parameter. With the following values for a and Q:

$$T^* < 263.15 \text{ K} \quad a = 1.14 \times 10^{-5} \text{ Pa}^{-3}\text{year}^{-1}$$
$$Q = 60 \text{ kJmol}^{-1}$$
$$T^* \geq 263.15 \text{ K} \quad a = 5.47 \times 10^{10} \text{ Pa}^{-3}\text{year}^{-1}$$
$$Q = 139 \text{ kJmol}^{-1} \tag{2}$$

$A(T^*)$ lies within the bounds put forward by Paterson and Budd (1982).

For the sliding velocity $\vec{v}_b$, a generalised Weertman relation is adopted, taking into account the effect of the subglacial water pressure:

$$\vec{v}_b = A_s \frac{(\vec{\tau}_b)^p}{Z} \tag{3}$$

where $\vec{\tau}_b$ is the basal shear stress, $p = 3$, Z the reduced weight of the overlying ice column and A_s is the basal sliding parameter. Values for the parameters A_s (Eq. 3) and m (Eq. 1) are specified further in Tables 2 and 3.

Ice shelves are included for Antarctica by iteratively solving a coupled set of elliptic equations for ice-shelf spreading in two dimensions, including the effect of lateral shearing induced by sidewalls and ice rises. At the grounding line, longitudinal stresses are taken into account in the effective stress term of the flow law. The model simulates realistic grounding line movement during glacial–interglacial transitions that compare well with the recent results of Pollard and DeConto (2009).

The melt/runoff module is based on the positive degree-day method and is identical to the recalibrated version of Janssens and Huybrechts (2000). Following what has become standard practice in large-scale ice-sheet modelling, the melting rate is set proportional to the yearly sum of positive degree days (PDD) at the surface and to two independent PDD factors for ice and snow. The expected sum of positive degree days (EPDD) can conveniently be evaluated as:

$$\text{EPDD} = \sigma \sum_{1}^{12} 30 \left[0.3989 \, \exp\left(-1.58 \left| \frac{T_{\text{mon}}^{\text{sur}}}{\sigma} \right|^{1.1372} \right) \right.$$
$$\left. + \max\left(0, \frac{T_{\text{mon}}^{\text{sur}}}{\sigma} \right) \right] \tag{4}$$

where the standard deviation σ is for temperature with respect to the monthly mean surface temperature $T_{\text{mon}}^{\text{sur}}$ to account for the daily cycle and random weather

fluctuations. The model distinguishes between snow accumulation, rainfall and melt water runoff and takes into account the process of melt water retention by refreezing and capillary forces in the snow pack. The melt model is also implemented in AIS, but current Antarctic summer temperatures remain generally below freezing and surface melting is negligible. Because of their very low surface slopes, it is further assumed that any melt water produced on the surface of Antarctic ice shelves refreezes in situ at the end of the summer season, and therefore does not escape to the ocean.

Isostasy is taken into account for its effect on bed elevation near grounding lines and marginal ablation zones, where it affects ice sheet dynamics. It enables ice sheets to depress the underlying bed, which can increase their volume by 25–30% for the same surface elevation. The bedrock adjustment model consists of a viscous asthenosphere, described by a single isostatic relaxation time, which underlies a rigid elastic plate (lithosphere). In this manner, the isostatic compensation takes into account the effects of changing ice load within an area several hundred kilometres wide, giving rise to deviations from local isostatic equilibrium. The value for the flexural rigidity (1 × 10^{25} N m) corresponds to a lithospheric thickness of 115 km and the characteristic relaxation time for the asthenosphere is set at 3,000 years.

Both ice and bedrock models have a horizontal resolution of 10 km, with 31 vertical layers in the ice, and another 9 layers in the underlying bedrock to calculate the heat conduction in the crust. The latter ensures a spatially variable geothermal heat flux at the ice sheet base that depends on the thermal history of ice and rock. The 10 km grid resolution is considerably higher than the one of ice sheet components used in other coupled models (e.g. Mikolajewicz et al., 2007a; Vizcaíno et al. 2008, 2010) and allows to better model features on relatively small scale such as fast-flowing outlet glaciers and ice streams, through which most of the ice flow towards the margin occurs. AGISM has been validated against glacial–interglacial changes (e.g. Huybrechts 2002).

2.1 Climate–ice sheet interactions

AGISM and the other components of LOVECLIM exchange (seasonal) information once a year. A third order Lagrangian polynomial interpolation was chosen to smooth the climate fields that feed into AGISM, since the numerical grid of both ice sheets is much finer than that of the other components. ECBilt provides AGISM with downscaled monthly temperature anomalies and annual precipitation ratios that are superimposed on the present-day fields (reference period 1970–2000). In turn, AGISM calculates the snow and ice fractions and the

(smoothed) surface height of the ice sheets that feed into ECBilt. The model thus incorporates the necessary couplings to provide feedbacks between albedo and temperature changes and surface elevation and temperature changes.

The ice sheet model provides the ocean model CLIO with temporally and spatially varying freshwater flux produced by a number of processes: basal and surface melting of the ice sheet, runoff from ice-free land (Greenland only) and iceberg calving. Iceberg calving happens at a prescribed outer boundary and is incorporated as a latent heat flux at the ocean surface. The associated latent heat and freshwater fluxes are released in the first oceanic grid cell bordering the continent along the coast, meaning that iceberg drift is not taken into account.

Since the basal melting rate below the ice shelves arguably constitutes the most important environmental forcing for the AIS in case of moderate warming, the heat flux at the ice shelf base and corresponding melting is incorporated using a modification of the parameterization of Beckmann and Goosse (2003). The melt rate $M(t)$ is assumed proportional to the total heat flux entering the cavity under the ice shelves integrated all along the perimeter of Antarctica $Q^{net}(t)$ and inversely proportional to the ice-shelf area $A(t)$:

$$M(t) = \frac{Q^{net}(t) \, A_0}{Q_0^{net} \, A(t)} M_0 \tag{5}$$

where t is the time, $M_0 = 0.25$ m/year and A_0 and Q_0^{net} are reference ice-shelf area and heat flux at the beginning of the experiments, respectively. The underlying assumption is that much of the water in the cavity is recycled locally forming a semi-closed circulation cell. $Q^{net}(t)$ is estimated directly from the mean ocean temperature around Antarctica.

3 Experimental set-up

Because of the long response time scales associated with polar ice sheet evolution of the order of thousands of years, it is necessary to start the ice sheet calculations sufficiently back in time. To this end, both AISM and GISM were run on 10 km resolution from the Last Glacial Maximum (19 kyr BP) onwards for a simulation of the glacial–interglacial transition and all of the Holocene. Hence, the desired outcome of this spin-up procedure are GIS and AIS at 1500 AD that are not in steady state, but rather carry the long-term memory of their history with them. These ice sheet configurations were used from 1500 AD onward in the fully coupled LOVECLIM experiments.

The core model experiments are idealized $2 \times CO_2$ scenarios (2CO2) with a one percent increase of the CO_2 concentration from a pre-industrial value of 277.5 ppm until doubling, after which it is kept constant until the end of 1,000-year runs. Each experiment is accompanied by a control experiment (CCTL) with constant pre-industrial forcing for 1,000 years that enables us to analyse any background trend. Furthermore, we analyse freshwater forcing experiments where an anomalous flux of 0.2 Sv (FW02) is added to the North Atlantic (20°–50°N) for 1,000 years with otherwise constant pre-industrial forcing. This represents a commonly used water hosing experiment to study the sensitivity of the MOC to freshwater perturbations (e.g. Stouffer et al. 2006), even though our forcing amplitude is relatively high. All experiments are performed both with a model version with fixed ice sheets (ECVL) and with the fully coupled LOVECLIM in order to compare results and study the impact of including dynamic ice sheets in the model.

The long response time scale of the ice sheets implies that equilibrium simulations with LOVECLIM for the pre-industrial climate are not well defined. While the ECVL scenario runs (2CO2, FW02) are started from a pre-industrial equilibrium, we run the fully coupled LOVECLIM from 1500 AD for 500 years under pre-industrial forcing in order to reduce the model coupling drift for the subsequent transient experiments starting in 2000 AD. A small adjustment of the climate model when ice sheets are first introduced in 1500 AD is sufficiently damped after the 500-year spin-up experiment.

4 Model climate sensitivity

To characterise the response of the model to the prescribed CO_2 forcing, we define the index $CS_{eff}^{1,000}$ as 'effective climate sensitivity' (Murphy 1995; Cubasch et al. 2001) after 1,000 years in experiment 2CO2. This definition runs in parallel with the IPCC AR4 definition (Randall et al. 2007), taking into account a specific cryospheric time scale of 1,000 years, when both major ice sheets are still present and contribute to climate feedbacks. This choice is guided by the fact that the two other IPCC AR4 definitions of equilibrium climate sensitivity (ECS) and transient climate response (TCR) (Cubasch et al. 2001; Randall et al. 2007) are not well suited either for our models including dynamic ice sheets (ECS) or for the time scale under consideration here (TCR). We compute $CS_{eff}^{1,000}$ following the notation of Gregory et al. (2002):

$$CS_{eff}^{1,000} = Q_{2x}/\lambda, \tag{6}$$

where $Q_{2x} = 3.78$ Wm^{-2} is the radiative forcing that results from a doubling of the CO_2 concentration in our model and λ can be calculated as

$$\lambda = \frac{Q_{2x} - F^{1,000}}{\Delta T^{1,000}} \qquad (7)$$

$F^{1,000}$ and $\Delta T^{1,000}$ are ocean heat uptake in Wm^{-2} and surface temperature change at year 1,000 of our model experiments, respectively. The resulting $\mathrm{CS}_{\mathrm{eff}}^{1,000}$ is consequently a measure of the strength of the feedbacks active on millennial time scales, which is the desired outcome. Note that latent heat transfer associated with ice sheet melting is at least an order of magnitude lower than ocean heat uptake and is therefore not taken into account here. In the following we will use the terms 'climate sensitivity' and $\mathrm{CS}_{\mathrm{eff}}^{1,000}$ interchangeably.

5 Parameter sets

In order to study the effect of including fully interactive ice sheets on climate sensitivity for a wide range of possible model responses, we use the methodology of an ensemble of different model versions. The ensemble is realized by selecting model parameter sets that produce reasonable simulations of the present-day climate and the climate evolution over the last millennium while yielding contrasted results for climate change scenarios. The parameter selection was done separately for different model components within realistic uncertainty bounds based on expert judgement (Loutre et al. 2010). Similar approaches include sampling a chosen range of the model's parameter space according to a Monte Carlo scheme (e.g. Knutti et al. 2002; Schneider von Deimling et al. 2006).

5.1 Climatic parameter sets

For the climatic component including atmosphere and ocean, we identified several sets of parameter values (Table 1) chosen within their range of uncertainty (cf. Goosse et al. 2007).

Table 1 Parameter selection for all nine 'climatic' parameter sets

Name	l2	l4	amplw	$\exp_{lw}$	albocef	albice	avkb	CorA
E11	0.125	0.070	1.00	0.3333	1.000	0	1.0	−0.0850
E12	0.120	0.067	1.00	0.4	0.900	0	2.0	0.0000
E21	0.125	0.070	1.00	0.4	0.900	0	1.5	−0.0850
E22	0.125	0.070	1.00	0.4	0.900	0	1.5	−0.0425
E31	0.131	0.071	1.00	0.5	0.950	0	2.5	−0.0850
E32	0.125	0.070	1.05	0.5	0.900	0	1.5	−0.0425
E41	0.131	0.071	1.10	0.5	0.900	0	2.5	−0.0850
E51	0.131	0.071	1.30	0.5	1.050	0.02	2.0	−0.0850
E52	0.125	0.070	1.30	0.5	1.000	0.02	1.5	−0.0425

See text for details

The first digit in the model name increases with increasing $\mathrm{CS}_{\mathrm{eff}}^{1,000}$ of the model, while the second indicates low (1) or high (2) MOC sensitivity to freshwater perturbations. The two parameters l2 and l4 are applied in the Rayleigh damping term of the equation of quasi-geostrophic potential vorticity in the atmospheric model. l2 corresponds to the 500–800 hPa layer of the model, while l4 corresponds 200–500 hPa layer (see equation 1 of Opsteegh et al. (1998) and equation 1 of Haarsma et al. (1996). The simple long-wave radiative scheme of LOVECLIM is based on an approach termed the Green's function method (Chou and Neelin 1996; Schaeffer et al. 1998). The scheme could be briefly represented for clear-sky conditions by the following formula for all the model levels:

$$F_{\mathrm{lw}} = F_{\mathrm{ref}} + FG(T', GHG') + G1 \cdot amplw \cdot (q')^{\exp_{lw}}, \qquad (8)$$

where F_{lw} is the long-wave flux, F_{ref} a reference value of the flux when temperature, humidity and the concentration of greenhouse gases are equal to the reference values, FG a function, not explicitly described here, allowing to compute the contribution associated with the anomalies compared to this reference in the vertical profile of temperature T' and in the concentrations of the various greenhouse gases in the atmosphere GHG'. The last term represents the anomaly in the long-wave flux due to the anomaly in humidity q'. The coefficients F_{ref}, $G1$ and those included in the function FG are spatially dependent. All the terms have been calibrated to follow as closely as possible a complex general circulation model long-wave scheme (Schaeffer et al. 1998), but large uncertainties are of course related to this parameterisation, in particular as the model only computes one mean relative humidity between the surface and 500 hPa, the atmosphere above 500 hPa being supposed to be completely dry. The albedo of the ocean in LOVECLIM depends on the season and on the location. At each time step, it is multiplied by albcoef in the experiments analysed here. For a typical albedo of the ocean of 0.06, using a value of 1.05 for albcoef increases the value of the albedo to 0.063. The albedo of the sea–ice (albice) is based on the scheme of Shine and Henderson-Sellers (1985), which uses different values for the albedo of snow, melting snow, bare ice and melting ice. For thin ice, the albedo is also dependent of the ice thickness. If albice is different from zero in the experiments discussed here, the value of the albedo in the model is increased by albice for all the snow and ice types. As explained in detail in Goosse et al. (1999), the minimum vertical diffusion coefficient in the ocean follows a vertical profile similar to the one proposed by Bryan and Lewis (1979). The coefficient avkb is a scaling factor that multiplies the minimum values of the vertical diffusion at all depths. A value of avkb of 1 (1.5, 2, 2.5) corresponds to a minimum background vertical

diffusivity in the thermocline of 10^{-5} m^2/s (1.5×10^{-5}, 2.0×10^{-5}, 2.5×10^{-5} m^2/s). As ECBILT systematically overestimates precipitation over the Atlantic and Arctic Oceans, it has been necessary to artificially reduce the precipitation rate over the Atlantic and Arctic basins (defined here as the oceanic area north of 68°N). The corresponding water is dumped into the North Pacific, a region where the model precipitation is too weak (Goosse et al. 2001). CorA corresponds to the fractional reduction of precipitation in the Atlantic. In LOVECLIM1.1 (this study), the Coriolis term in the equation of motion is computed in a fully implicit way because the semi-implicit scheme used for this term in LOVECLIM1.0 (Driesschaert et al. 2007; Swingedouw et al. 2008) induced too much numerical noise. The older scheme has been kept here in experiment E11 only, in order to have an easier comparison with the results of LOVECLIM1.0, which shares many climatic features with E11. Because of the larger implicit diffusion associated with this scheme, a lower value of the explicit diffusion avkb is applied in E11.

5.2 Ice sheet parameter sets

For the Antarctic and Greenland ice sheets, we define three different parameter sets that control ice sheet sensitivity along the 'melting axis'. These three model versions of AGISM are referred to as 'low', 'medium, and 'high'. The 'medium' model versions are identical to the standard version of AGISM used so far in LOVECLIM, which was tuned to best reproduce the present-day ice sheets and their sensitivity to climate change. Tables 2 and 3 give an overview of the parameter values selected to this effect.

Surface melting and runoff in AGISM are linked to surface temperature through the positive degree-day factors and the standard deviation of temperature variations around the monthly mean in the degree-day model σ (Janssens and Huybrechts 2000), cf. Equation (4). In GISM, these parameters also influence the shape of the present-day ice sheet as surface runoff is an important ingredient of today's mass balance. Within our range of parameter variations the melting strength controls mainly the area of the ice sheet but not its central thickness. To compensate for the associated volume change, it is therefore necessary to make adjustments for the ice stiffness and the ability to slide by making concomitant changes in the flow enhancement factor and the basal sliding parameter. The latter parameters mainly control the height-to-width ratio, and thus ice thickness, but hardly affect surface area. It is not possible to find a parameter set that satisfies present-day constraints on both ice thickness and surface area when the melting strength is modified. For the LOVECLIM runs, the parameter sets were chosen in order to obtain the same Greenland ice volume as known from present-day observations. Likewise, the smaller area ice sheet corresponding to the higher melting parameters also has the highest central ice thickness. For the given forcing and time scale in our study, these differences constitute a minor perturbation and have no marked influence on the results.

The complication of finding parameters for the surface melt model to match the present-day ice sheet geometry is absent from AISM as surface runoff is negligible under the current climate. Instead, parameter variations that modify basal melting below Antarctic ice shelves were chosen to only introduce changes with respect to the present-day reference state. This enables to use the same initial start-up files for all three sensitivity versions of AISM. The sensitivity of the basal melting rate below the ice shelves to oceanic conditions is subject to very large uncertainties, as

Table 2 Parameter selection for three versions of AISM along the melting axis

Model	Basal melting below ice shelves (m year^{-1} i.e.)	EPPD standard deviation σ (°C)	Positive-degree-day factor for snow melting (m year^{-1} PDD^{-1} i.e.)	Positive-degree-day factor for ice melting (m year^{-1} PDD^{-1} i.e.)
'low'	Constant at 0.25	4	0.75*0.003	0.75*0.008
'medium'	According to net heat input below the cavity	4.5	0.003	0.008
'high'	Triple the amount of the 'medium' run	5	1.25*0.003	1.25*0.008

i.e. ice equivalent

Table 3 Parameter selection for three versions of GISM along the melting axis

| Model	Enhancement factor/ multiplier for the rate factor in the flow law	Basal sliding parameter (m^8 N^{-3} year^{-1})	EPPD standard deviation σ (°C)	Positive-degree-day factor for snow melting (m year^{-1} PDD^{-1} i.e.)	Positive-degree-day factor for ice melting (m year^{-1} PDD^{-1} i.e.)
'low'	1.25×3.5	1.25×10^{-10}	4	0.75 (0.003/0.91)	0.75 (0.008/0.91)
'medium'	3.5	1.00×10^{-10}	4.5	0.003/0.91	0.008/0.91
'high'	0.5×3.5	0.5×10^{-10}	5	1.25 (0.003/0.91)	1.25 (0.008/0.91)
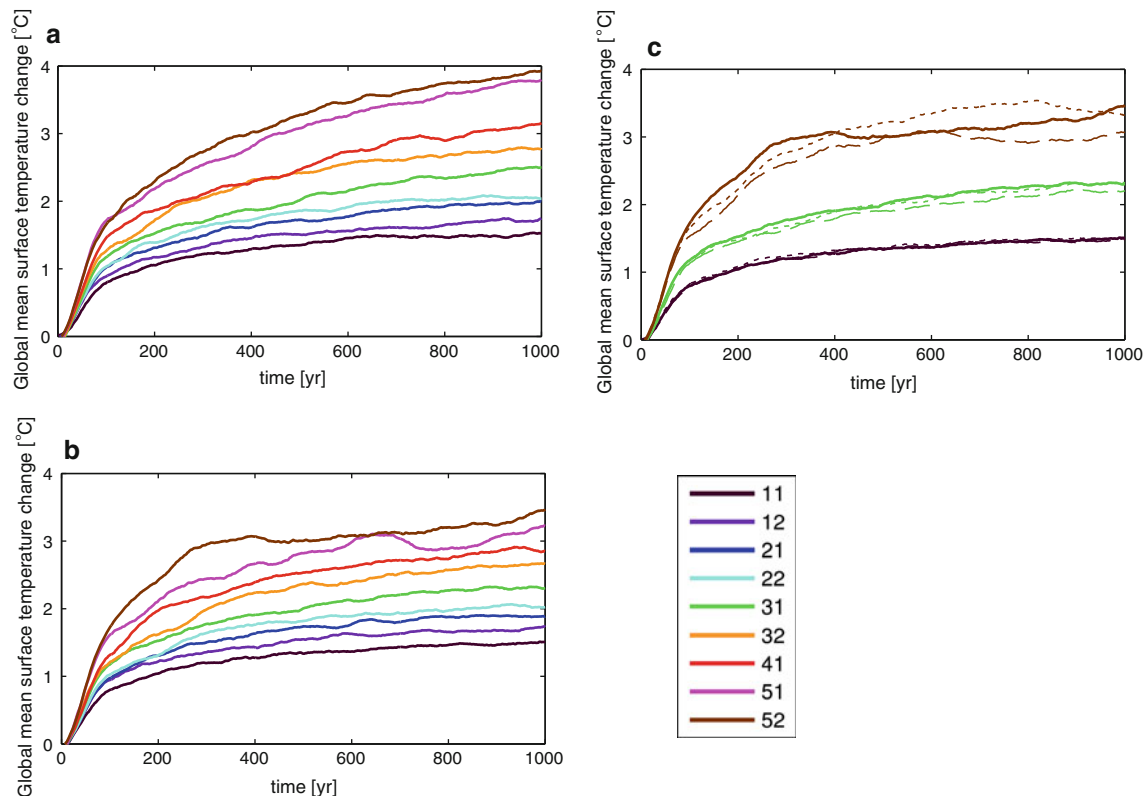
Fig. 3 Global mean surface temperature changes for experiments 2CO2 in ECVL (**a**), LOVECLIM with medium ice sheet sensitivity (**b**) and LOVECLIM models E11, E31 and E52 (**c**) for high (*dashed*), medium (*solid*) and low (*dotted*) ice sheet sensitivity. Time series are smoothed with a 25-year running mean

is its spatial distribution below the respective ice shelves (e.g. Holland et al. 2008). Therefore, our three parameter sets vary from a case with constant basal melting ('low') and a case with basal melting proportional to the oceanic heat input ('medium') to a case in which the oceanic heat input is tripled ('high'), cf. Table 2.

6 Results

The global mean surface temperature shows a rapid increase in the first 70 years for all parameter sets with ECVL experiment 2CO2 (Fig. 3a) while the CO_2 forcing is increasing. After that the rate of temperature change is levelling off. However, the warming still continues at the end of the 1,000-year experiment, when CO_2 levels have long stabilized, due to the long response time scale of the ocean. The strength of the temperature response scales with the experiment number, as intended in the choice of model parameters for the different parameter sets.

LOVECLIM first follows a similar response (Fig. 3b), but it is interesting to note that global mean surface temperature changes and the 'effective climate sensitivity' $CS_{eff}^{1,000}$ are generally lower when the ice sheets are included (Fig. 4). The strength of this mitigation effect scales

with the initial $CS_{eff}^{1,000}$ and furthermore depends on ice sheet sensitivity, with all high ice sheet sensitivity models showing the least warming of the three sets (Fig. 3c).

The mitigation of temperature changes in LOVECLIM is ultimately a negative feedback effect due to increasing freshwater fluxes from the melting ice sheets that affect the heat exchange in the ocean and at the sea-air interface. Stronger temperature response and stronger melting of the ice sheets both lead to stronger freshwater fluxes to the ocean and therefore increase the strength of the mitigation effect. In the following, we will study the different components responsible for this negative feedback mechanism in detail.

6.1 Polar temperature response

The change of mean surface temperature at the end of the 2CO2 LOVECLIM simulations over Greenland (Antarctica) lies between 4 and 10°C (4 and 12°C) for the different climatic parameter sets. This warming is between a factor of 2.3 and 3.2 (between 2.6 and 3.7 for Antarctica) higher than the global average because of the polar amplification seen in LOVECLIM. The amplification factors take different values when evaluated at different times of the 1,000 year runs but the model mean remains above 2.3 (2.5) at all times. Polar
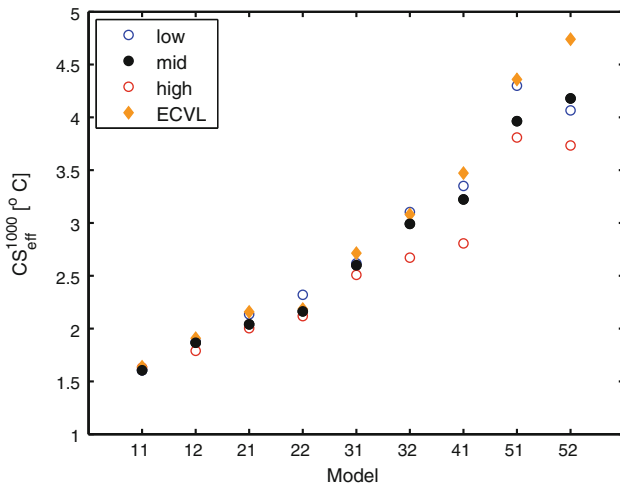
Fig. 4 Effective climate sensitivity after 1,000 years ($CS_{eff}^{1,000}$) of ECVL with fixed ice sheets (*orange diamonds*) and LOVECLIM with fully interactive Greenland and Antarctic ice sheet models (*circles*) with high (*red*), medium (*black*) and low (*blue*) ice sheet sensitivity
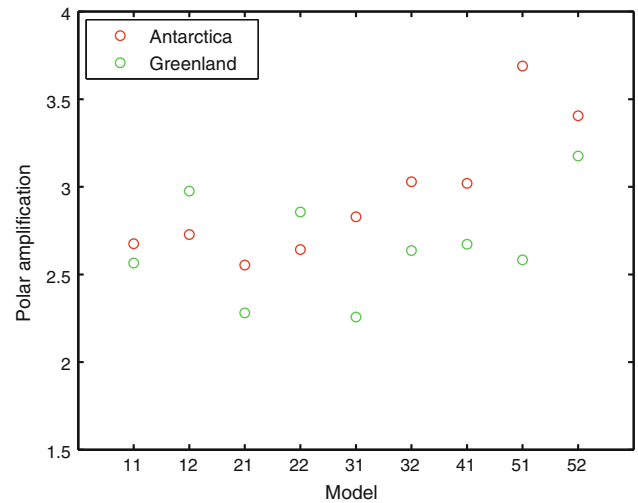

Fig. 5 Polar amplification factors over the Greenland (*green*) and Antarctic (*red*) ice sheets for LOVECLIM. For clarity only models with medium ice sheet sensitivity are displayed

amplification is a robust characteristic of the climate system but is stronger in LOVECLIM than in most other models. Gregory and Huybrechts (2006) found a polar amplification for Greenland of typically around 1.5 for a representative suite of IPCC AR4 AOGCMs and a negligible amplification for Antarctica. The amplification factors in LOVECLIM (Fig. 5) do not show a relation to the climate sensitivity of the model or to the strength of the mitigation effect. But, the higher polar amplification of LOVECLIM combines with low climate sensitivity versions (E11, E12, E21, E22) to yield polar temperature changes for a given radiative forcing that are in line with more comprehensive AOGCMs, while models with higher climate sensitivity show a relatively stronger polar response.

6.2 Melting of the ice sheets

The temperature increase over the GIS leads to a considerable increase in the amount of melting. Surface melting constitutes the dominant component of freshwater flux from the GIS, which is steadily increasing in all but the highest sensitivity models (E51, E52). For these two parameter sets freshwater fluxes start to decrease in the last 150 years (Fig. 6a) because the ice mass is already strongly reduced. At the end of the simulation up to 65% of the ice is removed for models E51 and E52. This also shows that the time scale of 1,000 years chosen in this study represents an upper limit for observing a GIS related mitigation effect in these high sensitivity models. For longer simulations the freshwater fluxes from Greenland will further decrease with the melting of the remaining ice and ultimately equal the continental runoff from land when no ice is left to melt.
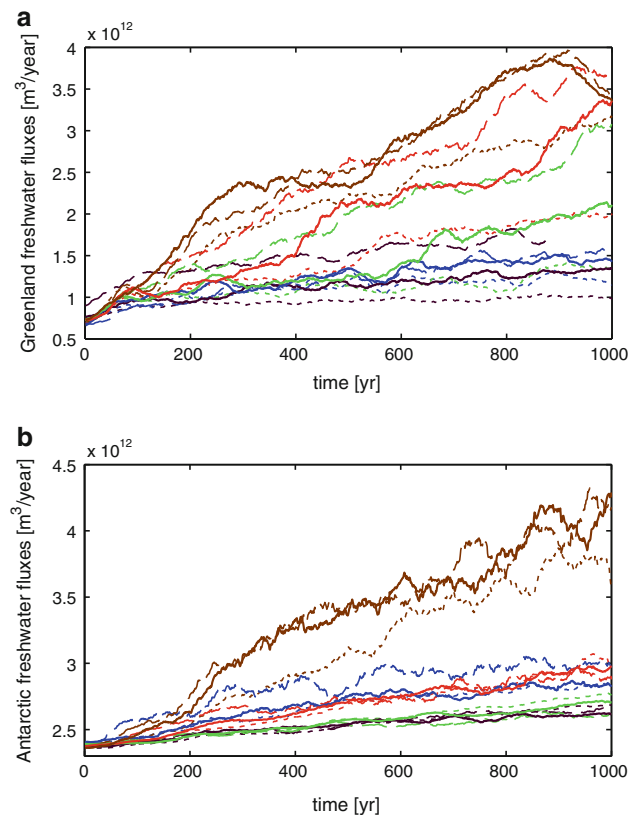

Fig. 6 Total freshwater fluxes from the GIS (**a**) and AIS (**b**) in experiment 2CO2 for high (*dashed*), medium (*solid*), and low (*dotted*) ice sheet sensitivity. For clarity only models E11, E21, E31, E41 and E52 are displayed. For colour legend see Fig. 3. Time series are smoothed with a 25-year running mean. A volume of 4×10^{12} m^3/year equals 0.13 Sv

In contrast, freshwater fluxes from the AIS are continuously increasing in all experiments (Fig. 6b). Iceberg calving, which accounts for most of the 2.3×10^{12} m^3/year flux at the beginning of the experiments does not show strong changes over the course of the experiments. But surface warming leads to a steady increase of ablation, which is negligible at the beginning of the experiments and becomes more and more important. Its increase is still ongoing with an almost constant rate at the end of the experiments and dominates changes in the total freshwater flux. This indicates that the AIS is far from equilibrium with the imposed warming even long after the forcing has stabilized. In fact, very long time-scales of the order of 10^4 years are required before the AIS eventually reaches a new steady state with less ice.

6.3 Influence of freshwater fluxes on surface temperature

We study the role of freshwater fluxes from the ice sheets exemplary for model E31 by means of 2CO2 experiments in which those fluxes have been suppressed in the Northern Hemisphere (NOFN), in the Southern Hemisphere (NOFS) and globally (NOFW). In order to separate their effect we only suppress freshwater fluxes, while changes in elevation and albedo due to ice sheet evolution are still taken into account. This is in contrast to Swingedouw et al. (2008) who also suppress changes in elevation and albedo.

The global mean surface temperature change in scenario 2CO2 (Fig. 7a) is strongest for ECVL (orange) and NOFW (green), followed by NOFN (red) and NOFS (blue) and finally by LOVECLIM (black). A LOVECLIM control experiment with fixed CO_2 concentration (CCTL, grey line) shows that there is no discernible model drift over the course of the experiments. The relative cooling (after 1,000 years) compared to ECVL is 0.16°C for NOFS, 0.14°C for NOFN and 0.23°C for LOVECLIM. This shows that freshwater fluxes from both ice sheets are responsible for attenuating the global temperature response in our model. The relative importance of the Northern Hemisphere is slightly higher in this model version and considerably higher for similar experiments with model version E51 (not shown).

Differences between LOVECLIM and NOFS are due to additional melt water fluxes from the Antarctic ice sheet in LOVECLIM that perturb the Antarctic surface waters, which leads to a stronger halocline with reduced vertical heat exchange. A resulting local decrease of the surface temperature is further amplified by the sea-ice-albedo and -insulation feedbacks (cf. Swingedouw et al. 2008).

The responsible mechanism for the relative cooling in LOVECLIM originating in the Northern Hemisphere can be found in the response of the MOC to increasing freshwater
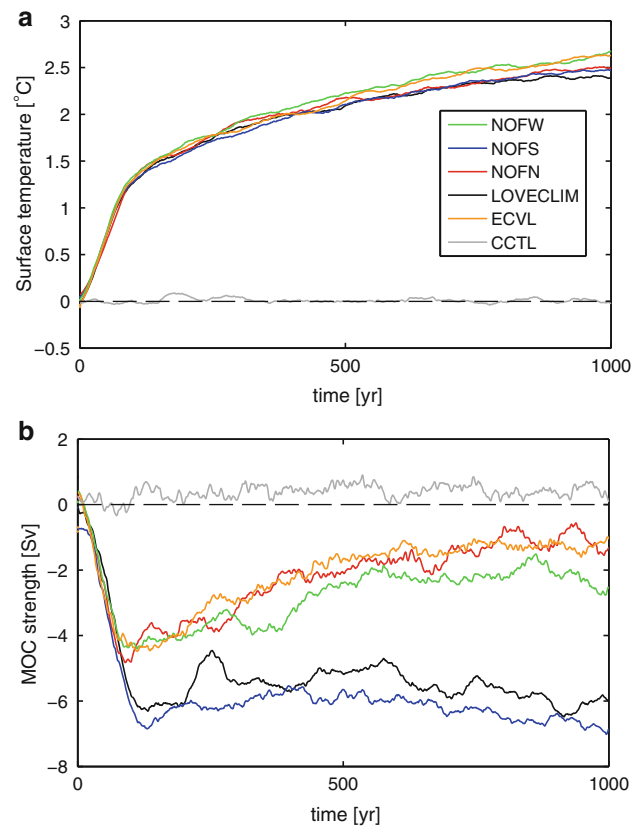

Fig. 7 Surface temperature changes (**a**) and MOC strength changes (**b**) in 2CO2 experiment for LOVECLIM model version E31 'medium' (*black*) and when freshwater fluxes from the ice sheets have been suppressed in the Northern Hemisphere (*red*), in the Southern Hemisphere (*blue*) and globally (*green*). Additionally displayed is the same 2CO2 experiment of ECVL (*orange*) and a LOVECLIM control simulation (*grey*) with fixed CO_2 concentration. The dashed line gives the long-term average of the ECVL control simulation. Time series are smoothed with a 25-year running mean

flux in the northern North Atlantic. While the MOC strength initially decreases in all experiments due to the thermal effect of greenhouse warming (cf. Gregory et al. 2005), it recovers in NOFN, NOFW and ECVL but decreases more and remains at a lower strength for NOFS and LOVECLIM (Fig. 7b). These last two experiments include freshwater fluxes from the melting GIS and thus cause an additional haline response of the MOC, which combined is stronger and more persistent than the thermal only response in the other experiments. The weaker MOC is associated with reduced meridional heat transport and a local relative cooling of the northern North Atlantic (e.g. Stocker et al. 1992; Rahmstorf 1994), which is further amplified by sea–ice-albedo and -insulation feedbacks. Ultimately, the relative cooling is also visible in the global mean temperature and thus constitutes a reduction of climate sensitivity.

Note that a similar temperature response of ECVL and NOFW shows that the ice-albedo feedback due to removal

of ice cover from Greenland has a minor influence for this experiment and on the millennial time scale under consideration here. Given that the GIS area reduction by the end of this experiment is not more than 25%, the ice-albedo feedback can be expected to become important on much longer time scales.

6.4 Sea–ice response

The sea–ice response constitutes an important feedback mechanism for the mitigation effect observed in our model ensemble, because remaining sea–ice cover has a higher albedo and a weaker insulation effect than ice-free ocean. Changes in annual mean sea-ice cover after 1,000 years of experiment 2CO2 show in both hemispheres a strong dependence on climate and ice sheet sensitivity (Fig. 8). Consistent with the higher climate sensitivity, the ECVL models generally loose more sea–ice than the comparable LOVECLIM models, of which most high ice sheet sensitivity models show the lowest loss of sea-ice cover in both hemispheres.

7 Discussion

We have identified negative feedback mechanisms in both hemispheres that lead to reduced climate sensitivity when ice sheets are included in the model. The negative feedback mechanism in the Northern Hemisphere has been shown to increase as a function of increasing ice sheet sensitivity and of increasing climate sensitivity of the model itself. Since the MOC plays an important role for differences of the global temperature response between ECVL and LOVECLIM, it is interesting to note that the MOC sensitivity itself is affected when including dynamic ice sheet models. We measure MOC sensitivity as the decrease in percent of the maximum value of the MOC stream function below the Ekman layer in the Atlantic Ocean after 1,000 years in experiment FW02. Most LOVECLIM models exhibit a lower MOC sensitivity than the corresponding ECVL versions (Fig. 9). This is due to the fact that weakening of the MOC results in a local cooling over Greenland, which forms part of a negative feedback mechanism. Melt water fluxes from the GIS that add to the prescribed anomalous fluxes are mitigated by temperature decreases over the ice sheet. An exception is model E11 with a stronger MOC sensitivity in LOVECLIM compared to ECVL, which is due to its rather weak initial MOC sensitivity in ECVL that prohibits a considerable cooling effect.

Since the feedback is effectuated by a weakening of the MOC by freshwater fluxes, it may be expected that the strength of the mitigation effect increases with increasing
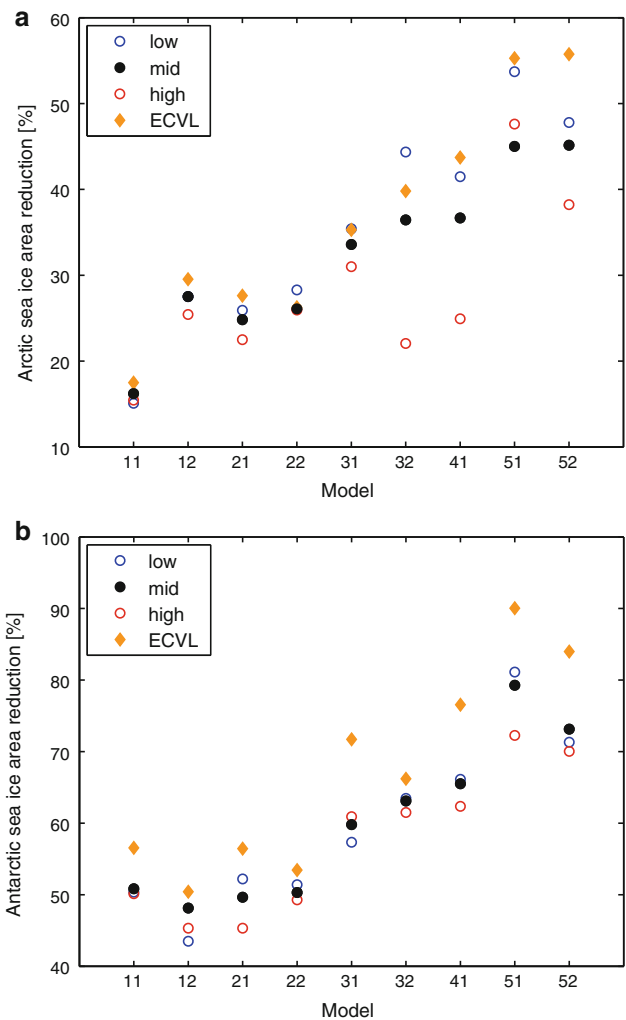
Fig. 8 Reduction of Arctic (**a**) and Antarctic (**b**) annual mean sea–ice area at the end of 2CO2 experiments for ECVL (*orange diamonds*) and LOVECLIM (*circles*) with high (*red*), medium (*black*) and low (*blue*) ice sheet sensitivity

sensitivity of the MOC to freshwater forcing (Fig. 9). In fact the contrary seems to be the case. This can be explained by the fact that MOC sensitivity in our model is strongly controlled by reducing the parameterized moisture transport out of the Atlantic (CorA), which brings the MOC closer to its bifurcation point. Higher MOC sensitivity in our model ensemble is therefore associated with a weaker initial MOC, which also means that differences in meridional heat transport that can be evoked by further weakening will be smaller. Higher MOC sensitivity therefore does not lead to a stronger mitigation effect in our model ensemble. Since MOC sensitivity to freshwater forcing varies strongly between different Earth system models (e.g. Stouffer et al. 2006), the magnitude of the mitigation effect can be expected to differ in other models.

LOVECLIM exhibits a relatively strong polar amplification compared to most other models, which increases the
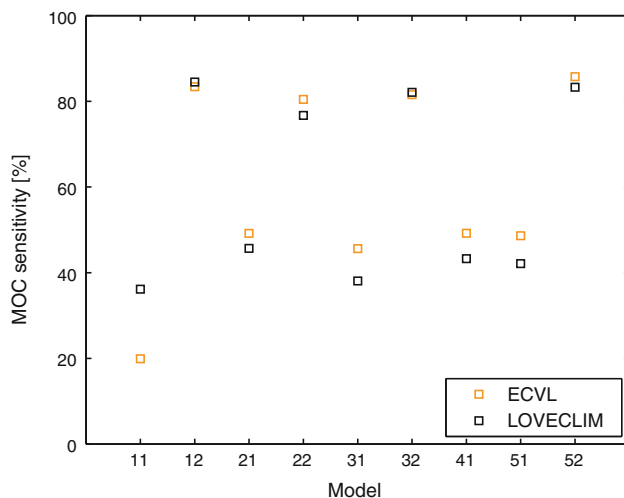
Fig. 9 MOC sensitivity differences between ECVL (*orange*) and LOVECLIM (*black*). See text for details. For clarity, only medium ice sheet sensitivity models are shown

magnitude of polar temperature changes and thus ice sheet melting in our experiments. This is particularly the case for the Antarctic where most comprehensive AOGCMs do not show a dominant polar amplification (e.g. Gregory and Huybrechts 2006). In contrast, the AIS response and the corresponding amount of freshwater fluxes for our models is probably an underestimate in case the large ice shelves would break up and calving could take place at grounding lines. These effects are not well represented in the current ice sheet model, which was developed for generally colder conditions with ice shelves present. For the high sensitivity models, it seems unlikely that the large ice shelves can be sustained, and they may well disintegrate after 500–1,000 years (Warner and Budd 1998). Higher order dynamical effects that are not included in the current generation of large-scale ice sheet models have been speculated to cause an acceleration of ice flow (e.g. Alley et al. 2005). If this should be the case, the ice sheets' response for a given warming would generally be underestimated.

On the millennial time scale under consideration here, the relative importance of the ice-albedo feedback due to partial removal of the GIS is negligible. This can be seen in a similar temperature response of ECVL and NOFW shown for model version E31, where the only difference between them is the albedo variation. This finding appears to be consistent with results from Vizcaíno et al. (2008) that suggest a threshold for the influence of the ice-albedo feedback when 3/4 of the original volume of the ice sheet is removed. For the extreme examples of our model ensemble, the GIS looses up to 65% of its original volume and 60% of its area until the end of the 1,000-year 2CO2

experiments, which is still below the proposed threshold. For even stronger forcing or on longer time scales, the positive ice-albedo feedback has to be expected to counter the mitigation effect, which will decrease by itself when most ice is removed and freshwater fluxes are strongly reduced.

On a longer multi-millennial time scale, which is set by the amount of ice sheet melting, the Northern Hemisphere mitigation effect can be considered as a transient phenomenon, because the GIS ultimately vanishes, freshwater fluxes consequently decrease and the MOC recovers. The Southern Hemisphere counterpart is also transient, but time scales are much longer. Our experiments indicate that the AIS is far from equilibrium with the imposed warming and surface melting is increasing for all model versions at the end of the experiments at an almost linear rate. Consequently, the mitigation effect due to Antarctic freshwater fluxes will further increase as has been shown by Swingedouw et al. (2008) with an earlier version of LOVECLIM. Their results show, although not explicitly stated, that the mitigation effect in the Southern Hemisphere outlasts the one in the Northern Hemisphere.

8 Conclusions

We find that climate sensitivity of our models is reduced on a millennial time scale when including dynamic ice sheet models due to the effect of additional freshwater fluxes from the ice sheets. In the Northern Hemisphere, melt water induced MOC weakening and local relative cooling is amplified by sea–ice-related feedbacks. A similar mechanism in the Southern Hemisphere contributes to the mitigation, which has a smaller effect, but may become important for strong temperature forcing with considerable melt water fluxes from Antarctica. By using an ensemble of models with different parameter sets, we were able to assess the role of differences in model sensitivities that are poorly constrained and vary largely between models in the GCM and EMIC community. The described mitigation effect increases with ice sheet sensitivity and with the initial climate sensitivity of the model itself. We suggest that it is of great importance to be aware of this dynamical effect when including ice sheet models into global Earth system models, and also when using models where interactions with the ice sheets are not considered.

References

Alley R, Clark P, Huybrechts P, Joughin I (2005) Ice sheets and sea-level change. Science 310:456–460

Beckmann A, Goosse H (2003) A parameterization of ice shelf-ocean interactions for climate models. Ocean Model 5:157–170

Brovkin V, Ganopolski A, Svirezhev Y (1997) A continuous climate-vegetation classification for use in climate biosphere studies. Ecol Modell 101:251–261

Bryan K, Lewis L (1979) A water mass model of the world ocean. J Geophys Res 84(C5):2503–2517

Calov R, Ganopolski A, Claussen M, Petoukhov V, Greve R (2005) Transient simulation of the last glacial inception. Part I: glacial inception as a bifurcation in the climate system. Clim Dyn 24:545–561

Chou C, Neelin J (1996) Linearization of a long-wave radiation scheme for intermediate tropical atmospheric models. J Geophys Res 101(15):15,129–15,145

Cubasch U, Meehl GA, Boer GJ, Stouffer RJ, Dix M, Noda A, Senior CA, Raper S, Yap KS (2001) Projections of future climate change. In: Houghton JT, Ding Y, Griggs DJ, Noguer M, van der Linden PJ, Dai X, Maskell K, Johnson CA (eds) Climate change 2001. The scientific basis. Contribution of working group I to the third assessment report of the intergovernmental panel on climate change. Cambridge University Press, Cambridge, p 881

Driesschaert E, Fichefet T, Goosse H, Huybrechts P, Janssens I, Mouchet A, Munhoven G, Brovkin V, Weber SL (2007) Modeling the influence of Greenland ice sheet melting on the meridional overturning circulation during the next millennia. Geophys Res Lett L10707

Fichefet T, Morales Maqueda M (1997) Sensitivity of a global sea-ice model to the treatment of ice thermodynamics and dynamics. J Geophys Res 102:12,609–12,646

Fichefet T, Poncin C, Goosse H, Huybrechts P, Janssens I, Le Treut H (2003) Implications of changes in freshwater flux from the Greenland ice sheet for the climate of the 21st century. Geophys Res Lett 30:L1911

Goosse H, Fichefet T (1999) Importance of ice-ocean interactions for the global ocean circulation: a model study. J Geophys Res 104:23,337–23,355

Goosse H, Deleersnijder E, Fichefet T, England M (1999) Sensitivity of a global coupled ocean–sea-ice model to the parameterization of vertical mixing. J Geophys Res 104:13,681–13,695

Goosse H, Selten FM, Haarsma RJ, Opsteegh JD (2001) Decadal variability in high northern latitudes as simulated by an intermediate complexity climate model. Ann Glaciol 33:525–532

Goosse H, Driesschaert E, Fichefet T, Loutre M-F (2007) Information on the early Holocene climate constrains the summer sea ice projections for the 21st century. Clim Past 3:683–692

Goosse H, Brovkin V, Fichefet T, Haarsma R, Huybrechts P, Jongma J, Mouchet A, Selten F, Barriat PY, Campin JM, Deleersnijder E, Driesschaert E, Goelzer H, Janssens I, Loutre MF, Morales Maqueda MA, Opsteegh T, Mathieu PP, Munhoven G, Petterson JE, Renssen H, Roche D, Schaeffer M, Tartinville B, Timmermann A, Weber SL (2010) Description of the Earth system model of intermediate complexity LOVECLIM version 1.2. Geosci Model Dev Discuss 3:309–390

Gregory JM, Huybrechts P (2006) Ice-sheet contributions to future sea-level change. Philos Trans R Soc A 364:1709–1732

Gregory JM, Stouffer RJ, Raper SCB, Stott PA, Rayner NA (2002) An observationally based estimate of the climate sensitivity. J Clim 15:3117–3121

Gregory JM, Dixon KW, Stouffer RJ, Weaver AJ, Driesschaert E, Eby M, Fichefet T, Hasumi H, Hu A, Jungclaus JH, Kamenkovich IV, Levermann A, Montoya M, Murakami S, Nawrath S, Oka A, Sokolov AP, Thorpe RB (2005) A model intercomparison of changes in the Atlantic thermohaline circulation in response to increasing atmospheric CO_2 concentration. Geophys Res Lett 32:L12703

Haarsma RJ, Selten FM, Opsteegh JD, Lenderink G, Liu Q (1996) ECBILT, a coupled atmosphere ocean sea-ice model for climate predictability studies. KNMI, De Bilt, The Netherlands, 31 p

Holland PR, Jenkins A, Holland DM (2008) The response of ice shelf basal melting to variations in ocean temperature. J Clim 21:2558–2572

Huybrechts P (1990) A 3-D model for the Antarctic ice sheet: a sensitivity study on the glacial–interglacial contrast. Clim Dyn 5:79–92

Huybrechts P (1996) Basal temperature conditions of the Greenland ice sheet during the glacial cycles. Ann Glaciol 23:226–236

Huybrechts P (2002) Sea-level changes at the LGM from ice-dynamic reconstructions of the Greenland and Antarctic ice sheets during the glacial cycles. Q Sci Rev 21:203–231

Huybrechts P, de Wolde J (1999) The dynamic response of the Greenland and Antarctic ice sheets to multiple-century climatic warming. J Clim 12:2169–2188

Huybrechts P, Janssens I, Poncin C, Fichefet T (2002) The response of the Greenland ice sheet to climate changes in the 21st century by interactive coupling of an AOGCM with a thermomechanical ice sheet model. Ann Glaciol 35:409–415

Janssens I, Huybrechts P (2000) The treatment of melt water retention in mass-balance parameterizations of the Greenland ice sheet. Ann Glaciol 31:133–140

Johns TC, Gregory JM, Ingram WJ, Johnson CE, Jones A, Lowe JA, Mitchell JFB, Roberts DL, Sexton DMH, Stevenson DS, Tett SFB, Woodage MJ (2003) Anthropogenic climate change for 1860 to 2100 simulated with the HadCM3 model under updated emissions scenarios. Clim Dyn 20:583–612

Knutti R, Stocker TF, Joos F, Plattner G-K (2002) Constraints on radiative forcing and future climate change from observations and climate model ensembles. Nature 416:719–723

Loutre MF, Mouchet A, Fichefet T, Goosse H, Goelzer H, Huybrechts P (2010) Evaluating climate model performance with various parameter sets using observations over the last centuries. Clim Past Discuss 6:711–765

Mikolajewicz U, Gröger M, Maier-Reimer E, Schurgers G, Vizcaíno M, Winguth A (2007a) Long-term effects of anthropogenic CO_2 emissions simulated with a complex earth system model. Clim Dyn 28:599–633

Mikolajewicz U, Vizcaíno M, Jungclaus J, Schurgers G (2007b) Effect of ice sheet interactions in anthropogenic climate change simulations. Geophys Res Lett 34:L18706

Mouchet A, François L (1996) Sensitivity of a global oceanic carbon cycle model to the circulation and to the fate of organic matter: preliminary results. Phys Chem Earth 21:511–516

Murphy JM (1995) Transient response of the Hadley Centre coupled ocean–atmosphere model to increasing carbon dioxide. Part III: analysis of global-mean response using simple models. J Clim 8:496–514

Nakashiki N, Kim D-H, Bryan FO, Yoshida Y, Tsumune D, Maruyama K, Kitabata H (2006) Recovery of thermohaline circulation under CO_2 stabilization and overshoot scenario. Ocean Model 15:200–217

Opsteegh J, Haarsma R, Selten F, Kattenberg A (1998) ECBILT: a dynamic alternative to mixed boundary conditions in ocean models. Tellus 50:348–367

Paterson WSB, Budd WF (1982) Flow parameters for ice sheet modelling. Cold Reg Sci Technol 6:175–177

Pollard D, DeConto RM (2009) Modelling West Antarctic ice sheet growth and collapse through the past five million years. Nature 458:329–332

Rahmstorf S (1994) Rapid climate transitions in a coupled ocean-atmosphere model. Nature 372:82–85

Rahmstorf S, Ganopolski A (1999) Long-term global warming scenarios computed with an efficient coupled climate model. Clim Change 43:353–367

Randall DA, Wood RA, Bony S, Colman R, Fichefet T, Fyfe J, Kattsov V, Pitman A, Shukla J, Srinivasan J, Stouffer RJ, Sumi A, Taylor KE (2007) Climate models and their evaluation. In: Solomon S, Qin D, Manning M, Chen Z, Marquis M, Averyt KB, Tignor M, Miller HL (eds) Climate change 2007: the physical science basis. Contribution of Working Group I to the Fourth Assessment Report of the Intergovernmental Panel on Climate Change. Cambridge University Press, Cambridge

Ridley J, Huybrechts P, Gregory J, Lowe J (2005) Elimination of the Greenland ice sheet in a high CO_2 climate. J Clim 18:3409–3427

Schaeffer M, Selten F, van Dorland R (1998) Linking Image and ECBILT. National Institute for public health and the environment (RIVM), Bilthoven, The Netherlands, Report no 4815008008

Schneider von Deimling T, Held H, Ganopolski A, Rahmstorf S (2006) Climate sensitivity estimated from ensemble simulations of glacial climate. Clim Dyn 27:149–163

Shine KP, Henderson-Sellers A (1985) The sensitivity of a thermodynamic sea ice model to changes in surface albedo parameterization. J Geophys Res 90(D1):2243–2250

Stocker TF, Wright DG, Broecker WS (1992) The influence of high-latitude surface forcing on the global thermohaline circulation. Paleoceanography 7(5):529–541

Stouffer RJ, Yin J, Gregory JM, Dixon KW, Spelman MJ, Hurlin W, Weaver AJ, Eby M, Flato GM, Hasumi H, Hu A, Jungclaus JH, Kamenkovich IV, Levermann A, Montoya M, Murakami S, Nawrath S, Oka A, Peltier WR, Robitaille DY, Sokolov A, Vettoretti G, Weber SL (2006) Investigating the causes of the response of the thermohaline circulation to past and future climate changes. J Clim 19:1365–1387

Swingedouw D, Fichefet T, Huybrechts P, Goosse H, Driesschaert E, Loutre M-F (2008) Antarctic ice-sheet melting provides negative feedbacks on future climate warming. Geophys Res Lett 35:L17705

Vizcaíno M, Mikolajewicz U, Gröger M, Maier-Reimer E, Schurgers G, Winguth A (2008) Long-term ice sheet-climate interactions under anthropogenic greenhouse forcing simulated with a complex Earth System Model. Clim Dyn 31:665–690

Vizcaíno M, Mikolajewicz U, Jungclaus J, Schurgers G (2010) Climate modification by future ice sheet changes and consequences for ice sheet mass balance. Clim Dyn 34:301–324

Warner RC, Budd WF (1998) Modeling the long-term response of the Antarctic ice sheet to global warming. Ann Glaciol 27:161–168

Winguth A, Mikolajewicz U, Gröger M, Maier-Reimer E, Schurgers G, Vizcaíno M (2005) Centennial-scale interactions between the carbon cycle and anthropogenic climate change using a dynamic Earth system model. Geophys Res Lett 32:L23714